ratio lowers C_{m_q} values by about a factor of 2 for the unablative or solid wall model tests. These same no blowing runs indicated (C_{m_α} data not presented) that the effect of increased nose bluntness ratio is to translate the aerodynamic center aft about 0.10 diam.

It was assumed as a result of preliminary examination of the data that the primary reason for increased dynamic stability with mass addition to the boundary layer was an effective shape change. It was hypothesized that coating the aft portion of the model should add an effective "flare" to the cone and possibly increase both static and dynamic stability. Runs were made with only the aft portion of the cone coated. As the data demonstrate, when the model was released, it damped slightly for the first few seconds; then as the ablation material approached a full blowing rate, the motion began to diverge and continued to diverge steadily to the end of the run. Figure 2 also shows that injecting nitrogen gas through a porous nose has only a small effect on C_{m_q}. This gas was not phased with the oscillatory motion of the model and therefore does not simulate ablative phase lag experienced by windward-leeward oscillating ablative surfaces. The same pronounced effects obtained by ablation on the cone configurations are also seen on the slender cone-cylinder-flare shapes. Bluntness effects are similar also. Once again, coating the surface of the model aft of the center of rotation (i.e., center of gravity) produced dynamic instability.

Summary

In Ref. 2 it is hypothesized that, for certain re-entry shapes, e.g., "theoretically sharp" slender cones, transition may occur first at the base with accompanying increases in heating and (depending on the heat shield material) with an increase in the ablative blowing rate in this region and possible dynamic instability. Sufficient flight-test data of recent date exist to support this thought. Examination of the ablation tests made at FluiDyne indicates the degree of sensitivity of the damping derivative not only to the presence of ablation but also to its location, whether ahead or behind the center of gravity. Coating the entire model, or forward of the center of gravity, produces a dynamically stable configuration with $C_{m_q} + C_{m_{\dot\alpha}}$ values approaching those for flight test. Coating the rearward sections of a conic or cone-cylinder-flare produces a dynamically unstable vehicle.

If we combine the observed test results and available flight-test data with the transition hypothesis of Sacks and Schurmann,[2] then some of the aerodynamic phenomena associated with advanced re-entry bodies can be explained. As they point out by way of illustration, normal angle-of-attack convergence patterns can be expected during the high-altitude, laminar portion of the trajectory. This would correspond to ablation from the nose or forward sections of the wind-tunnel models, i.e., stabilized C_{m_q}, or convergence. As the vehicle descends further and approaches the transition Reynolds number regime, the angle-of-attack oscillatory pattern may blow up or converge at even a faster rate. Should the flow experience transition at the base first, higher heating rates will be experienced in this area than on the forward sections, and hence marked increase in ablation can be expected. In the tunnel tests, the ablative models coated on the aft sections diverged, i.e., C_{m_q} became positive. Should the flow undergo transition instantaneously, then dynamic instability will not occur and convergence rate will increase. This would correspond to the tunnel test with the ablative models completely coated.

The profound effect of ablation on aerodynamic damping shown in these tests demonstrates that an important physical phenomenon is acting which must be investigated further. Preliminary work has been started to formulate analytical expressions associated with boundary-layer effects on the pressure distributions over an ablating, oscillating body in hypersonic flow. It is also apparent from the analyses that, in order to obtain significant effects on dynamic stability, an aerothermo lag parameter may exist, and the magnitude and sign of this effect on C_{m_q} is dependent upon the center of gravity location. Should subsequent investigations prove the existence of an aerodynamic lag time due to ablation, then a significant parameter has been uncovered to explain behavior of slender re-entry vehicles.

References

1 Syvertson, C. A. and McDevitt, J. B., "Effects of mass addition on the stability of slender cones at hypersonic speeds," AIAA J. **2**, 939–940 (1963).

2 Sacks, I. and Schurmann, E. E., "Aerodynamic phenomena associated with advanced reentry systems," Avco-RAD-TM-63-79, pp. 18–22 (October 31, 1963).

Simplified Equations for Determining Propulsion System Specific Impulse

MARIO W. CARDULLO*
Bellcomm, Inc., Washington, D. C.

Nomenclature

C = const, in.²/lbm
F = thrust, lbf
I_{sp} = theoretical propellant specific impulse, lbf-sec/lbm
I_{ss} = propulsion system specific impulse, lbf-sec/lbm
I_{ssi} = subsystem "i" specific impulse, lbf-sec/lbm
I_t = total impulse, lbf-sec
K = factor less than or equal to unity to account for acceleration, flanges, and welds
M_g = gross stage mass, slugs
M_p = payload mass, slugs
n = number of modules
O/F = oxidizer to fuel weight ratio
P_c = combustion chamber pressure, psia
P = pressure, psia
R = gas constant of pressurant, in./°R
S = design stress, lbf/in.²
t = thickness, in.
t_B = burning time, sec
t_m = minimum wall thickness, in.
T = temperature, °R
v = velocity, fps
V = volume, in.³
α = weight ratio of expelled to total propellant originally in tanks (expulsion efficiency)
β = weight ratio of propellant trapped and/or lost by vaporization to total propellant originally in tanks
γ = ratio of specific heats
ϵ = expansion ratio
η = propellant performance efficiency
ξ = density factor defined in Table 1, lb/in.³
ρ = density, lb/in.³

Subscripts

B = bladder
F = fuel
G = pressurant
O = oxidizer
P = propellant
T = tank

VARIOUS techniques have been used in the past to compare and select propulsion systems. Williams[1] employed the ratio of total impulse to weight to compare various attitude control propulsion systems. A comparison based upon

Received April 1, 1964; revision received September 29, 1964.
* Member of Technical Staff. Member AIAA.

payload fraction (payload to gross weight) was used by Orr[2] in selecting upperstage propellants. Roberson[3] in his study of control systems used the inverse of Williams' function for system comparison.

The use of a propulsion system specific impulse (same as Williams' impulse to weight ratio) was shown by Ross[4] to offer a means of comparing diverse propulsion systems on a similar basis. The system specific impulse (I_{ss}) is defined as the ratio of total impulse to total propulsion system loaded weight. The system specific impulse offers a means to evaluate the useful total impulse achieved from any propulsion system. The velocity change from any stage can be shown to be a function of the system specific impulse and payload fraction[4] and can be written

$$\Delta v = gI_{ss} \ln(M_g/M_p) \tag{1}$$

The reciprocal of the system specific impulse can be shown to consist of the sum of the reciprocals of all the subsystem specific impulse (I_{ssi}) where

$$\sum_{i=1}^{a} I_{ssi} = \sum_{i=1}^{a} \frac{I_t}{W_i} \tag{2}$$

Thus by defining the subsystem specific impulse of components (i.e., tanks, engines, propellants, etc.) it can be possible to construct analytical models of various types of propulsion systems.

Table 1 presents a summary of simplified equations for determining subsystem specific impulse. The specific impulse of the pressurant is shown to be independent of the total impulse of the system but directly proportional to the usable specific impulse (I_{ssi}) of the propellant. The subsystem specific impulse for tanks is constant above a certain total impulse level. This level is determined primarily by the minimum fabricational wall thickness (t_m). This total impulse level is about 2000 to 10,000 lb-sec for earth storable propellants. Dividing the propulsion system into several identical smaller systems produces a modular propulsion

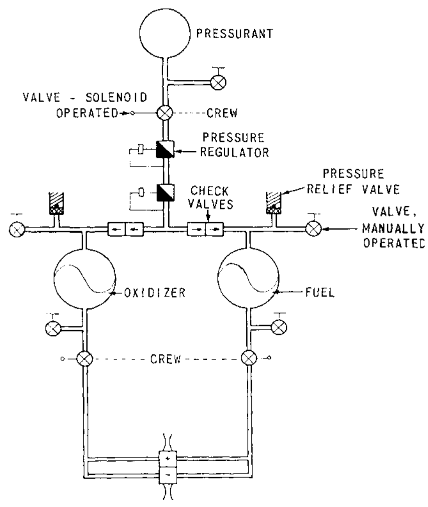

Fig. 1 Pressurization and propellant system schematic.

Table 1 Summary of subsystem equations[a]

SYSTEM OR COMPONENT	SPECIFIC IMPULSE	ASSUMPTIONS	REF.
TOTAL PROPULSION SYSTEM	$\frac{1}{I_{SS}} = \sum_{i=1}^{a} \frac{1}{I_{SSi}}$		
PROPELLANT	$I_{SS1} = (\alpha - \beta)\,\eta\, I_{SP}$		
PRESSURANT	$I_{SS2} = \left(\frac{R}{\gamma}\right)\left(\frac{T}{P_P}\right)\left(\frac{\langle\rho\rangle_P I_{SS1}}{\alpha}\right)$	$P_G V_G \approx \gamma P_P V_P$ INITALLY	6
EXPULSION BLADDERS	$I_{SS3} = \left[\frac{I_{SS1} \langle\xi\rangle_P}{6\alpha}\right]^{2/3} \left(\frac{I_T}{n\pi}\right)^{1/3} \frac{1}{(t\rho)_B}$	SPHERICAL BLADDERS, THICKNESS AND MATERIAL SIMILAR FOR BOTH FUEL AND OXIDIZER BLADDERS	
PROPELLANT TANKS FOR $I_T \le \left(\frac{32n}{3\alpha}\right)\left(\frac{O/F+1}{O/F}\right)\left(\frac{t_m S}{P}\right)^3_{PT} \rho_O I_{SS1}$	$I_{SS4} = \left[\frac{I_{SS1} \langle\xi\rangle_P}{6\alpha}\right]^{2/3} \left(\frac{I_T}{n\pi}\right)^{1/3} \left(\frac{K}{t\rho}\right)_{PT}$	SPHERICAL TANKS, THICKNESS AND MATERIAL SIMILAR FOR BOTH FUEL AND OXIDIZER TANKS	
$I_T \ge \left(\frac{32n}{3\alpha}\right)\left(\frac{O/F+1}{O/F}\right)\left(\frac{t_m S}{P}\right)^3_{PT} \rho_O I_{SS1}$	$I_{SS4} = \left[\frac{2 I_{SS1} \langle\rho\rangle_P}{3\alpha}\right]\left(\frac{SK}{P\rho}\right)_{PT}$	" " "	
PRESSURANT TANKS FOR $I_T \le \left(\frac{32n}{3\alpha}\right)\left(\frac{\pi}{\gamma}\right)\left[\frac{(t_m S)^3_{GT}}{P_G^2 P_P}\right] \langle\rho\rangle_P I_{SS1}$	$I_{SS5} = \left[\frac{I_{SS1} \langle\rho\rangle_P P_G}{6\alpha\gamma P_P}\right]^{2/3} \left(\frac{I_T}{n\pi}\right)^{1/3} \left(\frac{K}{t\rho}\right)_{GT}$	" " "	
$I_T \ge \left(\frac{32n}{3\alpha}\right)\left(\frac{\pi}{\gamma}\right)\left[\frac{(t_m S)^3_{GT}}{P_G^2 P_P}\right] \langle\rho\rangle_P I_{SS1}$	$I_{SS5} = \left[\frac{2 I_{SS1} \langle\rho\rangle_P}{3\alpha P_P}\right]\left(\frac{SK}{\rho}\right)_{GT}$	" " "	
ENGINE AND ACCESSORIES TURBOPUMP AND GAS GENERATOR	$I_{SS6} = \frac{I_T}{n\left[160 \log_{10} F - 575\right]}$		5
PRESSURE FED ABLATIVE ENGINE	$I_{SS7} = \frac{t_B}{\left[\frac{0.22}{P_C^{3/8}}\left(\frac{t_B^2}{I_T}\right)^{1/4} + \frac{(\epsilon - 40)}{200 P_C}\right] n}$	INCLUDES INJECTOR, ABLATIVE CHAMBER, NOZZLE EXIT SKIRT, THRUST-CHAMBER VALVE AND ACTUATOR, INJECTOR SIDE OF THRUST AND GIMBAL MOUNT, ABLATIVE MATERIAL TO EXIT AREA RATIO OF 8:1, TITANIUM TO FINAL EXIT AREA RATIO	5
REGENERATIVE COOLED ENGINE	$I_{SS7} = \frac{I_T^{0.2}\, t_B^{0.8}\, P_C^{0.14}}{0.151\, n\, \epsilon^{0.1}}$	DRY ENGINE WEIGHT, TURBOPUMP, GIMBAL	5
RADIATION COOLED ENGINE	$I_{SS8} = C\, t_B\, P_C$	90 TA-10W ALLOY, $\epsilon = 40$, N_2O_4 -AEROZINE 50 O/F = 2, C*EFF = 95%	7

[a] $\langle\xi\rangle_p = \frac{(O/F + 1)^{2/3}}{[(O/F)/\rho_O]^{2/3} + (1/\rho_F)^{2/3}}$; $\langle\rho\rangle_p = \frac{O/F + 1}{[(O/F)/\rho_O] + 1/\rho_F}$; $C = \frac{\text{in}^3}{\text{lbm}}$.

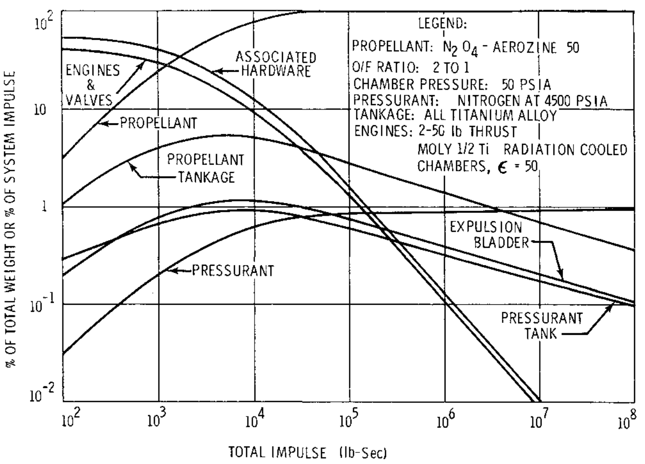

Fig. 2 Effect of total impulse on system component weights.

system. If the total amount of propellant is to be divided between "n" modules, then a weight penalty can be incurred. However, for medium to high total impulse ($I_t \leq$ 10,000 lb-sec, $F \leq$ 1000 lb), this penalty need not be significant, and for some cases it can be reduced by the lower weights associated with less propellant lines and manifolds. Depending upon the type of system, it may be possible to increase system reliability using an independent modular system. This penalty can be shown to be insignificant for high total impulse, low thrust systems ($I_i >$ 100,000 lb-sec, $F <$ 1,000 lb) since the propellant and pressurant specific impulse are independent of the number of modules (n).

Figure 1 shows a typical modular reaction control propulsion system, which was analyzed based upon the equations shown in Table 1. Figures 2 and 3 show the results of these calculations for various total impulses. In this case, the engines and associated hardware (values, lines, etc.) comprise a majority of the system weight for the low total impulse system ($I_t \leq$ 2000 lb-sec). As the total impulse increases, the majority of weight, as expected, is propellant. The pressurant approaches a maximum of 1% of the total weight as the total impulse is increased. If the subsystem specific impulse equations for the propellant and pressurant are compared, their ratio is found to be constant. The effect of total impulse on the over-all system specific impulse for the case analyzed is shown in Fig. 3. As the total impulse increases, the system impulse approaches asymptotically to the theoretical propellant specific impulse. The ratio of the system to propellant specific impulse is the propulsion system weight factor. Only for an ideal propulsion system does this factor equal unity; for any real system, this is always less than unity, but as the total impulse increases, this factor approaches asymptotically to unity.

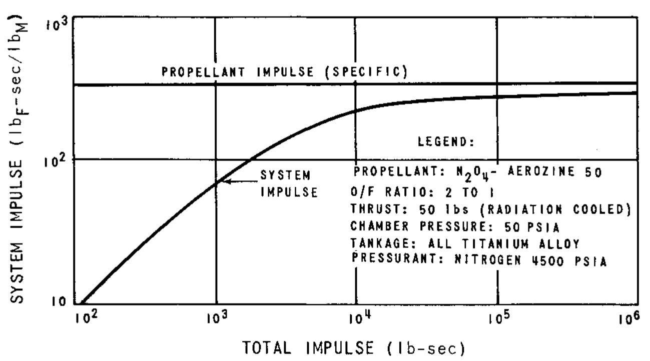

Fig. 3 Effect of total impulse upon system impulse.

References

[1] Williams, O. S., "Performance and reliability of attitude control rocket systems," ARS Preprint 952-59 (November 1959).

[2] Orr, J. A., "Some considerations for the selection of upper-stage propellants," Jet Propulsion Lab. TR 32-26 (April 1960).

[3] Roberson, R. E. (ed), "Methods for the control of satellites and space vehicles," *Sensing and Actuating Methods*, Vol. 7, Wright Air Development Div. WADD-TR-60-643 (July 1960).

[4] Ross, F. W., "Space system specific impulse," J. Aerospace Sci. **28**, 838–843 (1961).

[5] Tysdale, C. A., "Research study to determine propulsion requirements and systems for space missions," Aerojet-General Corp., Azusa, Calif., Rept. 2150 (December 1961).

[6] Barrere, M., Jaumotte, A., DeVeubeke, B. F., and Vandenkerckhove, J., *Rocket Propulsion* (Elsevier Publishing Co., Amsterdam, Holland, 1960), 1st ed., Chap. 7, pp. 475–480.

[7] Coulbert, C. D., "Selecting a thrust chamber cooling technique for spacecraft rocket engines," AIAA Preprint 63-241 (1963).

Application of Dynamic Programing to the Optimum Staging of Rockets

Anthony G. Lubowe*

Bell Telephone Laboratories, Inc., Whippany, N. J.

Nomenclature†

$f_k[V]$ = minimum weight of rocket k achieving velocity V
g = gravitational const (32.174 ft/sec^2)
I_i = specific impulse of stage i
N_i = ratio of initial thrust to weight of rocket i
w_i = initial gross weight of stage i
$\sigma_i w_i$ = total jettison weight of stage i
W_i = initial gross weight of rocket $i \equiv W_{i+1} + w_i$
r_i = burnout mass ratio $= W_i/(W_{i+1} + \sigma_i w_i)$
v_i = velocity added during stage i
n = number of stages
W_L = payload weight $\equiv W_{n+1}$
V_{bo} = actual burnout velocity
V_t = design velocity $= V_{bo}$ plus losses

Introduction

THE use of the dynamic programing technique to optimize the staging of rockets was proposed by Ten Dyke[1] several years ago. Recently, Fan and Wan[2] applied a discrete version of the maximum principle to the same problem. They claim that their solution is computationally superior to that of Ten Dyke. My own admittedly limited experience with the use of dynamic programing would lead me to agree with them if they were considering a problem of the type usually treated by the calculus of variations. However, dynamic programing may sometimes be useful computationally for the

Table 1[a] Saturn C-5 vehicle

Stage, i	I_i, sec	Thrust, lb	Propellant weight, lb
1	300	7500 × 10^6	4400 × 10^6
2	400	1000	900
3	400	230	230

[a] W_L = 100,000 lb ond V_{bo} = 36,000 fps.

Received June 11, 1964; revision received July 6, 1964. The author is grateful to F. T. Geyling for suggesting the problem, to J. H. W. Unger and D. van Z. Wadsworth for helpful discussions, and to A. Anastasio for the computer programs used for the numerical examples.

* Member of Technical Staff, Analytical and Aerospace Mechanics Department. Member AIAA.

† We will use Ten Dyke's original notation although it differs somewhat from that of Fan and Wan.